MOX-Report No. 48/2022

A wavelet-mixed landmark survival model for the effect of short-term oscillations in longitudinal biomarker's profiles

Gregorio, C.; Barbati, G.; Ieva, F.

MOX, Dipartimento di Matematica
Politecnico di Milano, Via Bonardi 9 - 20133 Milano (Italy)

mox-dmat@polimi.it http://mox.polimi.it

A wavelet-mixed landmark survival model for the effect of short-term oscillations in longitudinal biomarker's profiles

Gregorio C.[1,2], Barbati G.[1], Ieva F.[2,3]

[1] Biostatistics Unit, Department of Medical Sciences, University of Trieste, Via Valerio 4\1, Trieste 34100, Italy,

[2] MOX - Modelling and Scientific Computing, Department of Mathematics Politecnico di Milan, Piazza Leonardo Da Vinci 32, Milan 20123, Italy,

[3] HDSC, Health Data Science Center, Human Technopole, Viale Rita Levi Montalcini 1, Milan 20157, Italy.

Summary

Statistical methods to study the association between a longitudinal biomarker and the risk of death are very relevant for the long-term monitoring of frail subjects. In this context, sudden crises can cause the biomarker to undergo very abrupt changes. Although these oscillations are typically short-term, they often contain relevant prognostic information for the survival endpoint of interest. We propose a method that couples a linear mixed-model with a wavelet smoothing to extract both the long-term component and the short-term oscillations from the individual longitudinal biomarker profiles. We then use them as predictors in a landmark survival model to study their dynamic association with the risk of death. To illustrate the method, we use the clinical application which motivated our work, i.e., the monitoring of potassium in Heart Failure patients. The dataset consists of real-world data coming from the integration of Administrative

Health Records with Outpatient and Inpatient Clinic E-chart. Our method not only allows us to identify the short-term oscillations but also reveals their prognostic role in predicting the risk of death, according to their duration and, demonstrating the importance of including such short-term oscillations into the modeling. Compared to standard landmark analyses and joint models, the proposed method achieves higher predictive performances. In the context of the potassium monitoring, our analysis has important clinical implications since it allows us to derive a dynamic score that can be used in clinical practice to assess the risk related to an observed patient's potassium trajectory.

Key words: Monitoring of biomarkers, Survival analysis, time-dependent covariates, Heart Failure

1. Introduction

In many chronic diseases, patient's disease progression and status can be monitored over time through easily measured biomarkers. Medical decisions regarding treatments are often made on the basis on such monitoring. Hence, it is important to have quantitative tools to exploit information given by such measurements. Since the final goal of medical decisions is the minimization of the risk of adverse events such as hospitalizations or death, survival models are very often the building blocks of such tools. Recently two methods have been in widespread use for the modeling of longitudinal internal time-dependent covariates and survival: joint models and landmark models. In joint models the longitudinal biomarker process is modeled through linear mixed effects models which allow to consider the subjects' specific trajectories of the biomarker through the inclusion of random effects into the model. These latent variables are used to model the effect of unobserved variables that are responsible of subjects' deviation from the overall mean trajectory specified through the fixed effects (Tsiasis Anastasios A. and Davidian Marie, 2004). Versions of landmarking using linear mixed effect models have also been proposed to estimate the value

of the biomarkers at landmark times when the latter are different from measurement times and hence take into account measurement error (Rizopoulos *and others*, 2017). Much of the research in this context has been devoted to studying and comparing these two different approaches for modeling time-dependent covariates and the survival (Rizopoulos *and others*, 2017; Ferrer *and others*, 2019) and to explore and assess different associations structures between the two processes in joint models (Papageorgiou *and others*, 2019). One of the main advantages of modelling the longitudinal process of the biomarker is that we can study the relationship between the rate of change of the biomarker and the time-to-event process. However, a limitation of existing methods is that they don't take into account that the time scale of the survival process is very different from the time scale at which changes in the biomarkers happen in the human body. While in observational studies with the survival as the outcome of interest the follow-up period can be very long (e.g. years), intervals of measurements times are highly irregular because they depend of the clinical requirements. For example, during drugs up-tritation or acute disease periods more frequent measurements are required. As a consequence, such data is characterized by a very high observation period/time-between-measurements ratio. Sudden changes in biomarkers are very often important from a prognostic point of view. However, linear mixed effects model consider transient changes as measurement error when the length of the follow-up is much greater then their duration. Therefore, both joint models and landmark mixed models implicitly make a strong assumption, i.e., that short-term oscillations in biomarkers are either not present or they don't have effect on the risk of adverse events.

In this article we propose a novel approach to study the association between a continuous time-dependent longitudinal covariate and a time-to event outcome in order to overcome this limitation. Our method allows to identify and study the role of the short-term oscillations of the biomarker over time via a wavelet based functional approach and to set up a dynamic monitoring tool to support clinical decision making. The method is based on coupling a linear mixed effect model

with a wavelet filter. The first allows to identify the effect of fixed covariates and the long-term effect of time. On the other hand, the wavelet filter is used to identify the subject-specific short-term oscillations. The main idea is to combine a between-subjects model with a within-subject method such as a wavelet transform to obtain a functional and subject-specific representation of the biomarker trajectory over time. Wavelet filters are common methods in time-series analysis (Nason and Von Sachs, 1999) and signal processing (Unser and Aldroubi, 1996) to extract relevant features from the data and to remove noise and they have the advantage of identifying changes happening at different frequencies. Moreover, Functional Data Analysis (Ramsay and Silverman, 2005) offers methods to obtain functional objects from discrete and noisy longitudinal data and its application on time-dependent biomarker covariates offers a novel approach to extract biomarkers behaviors over time not observable with other methods.

In this article we tackle the problem of dynamically monitoring potassium in heart failure patients in order to provide support to clinical decisions. Heart Failure is a consequence of many cardiovascular diseases. In this chronic disease mortality and hospitalization rates remain high, despite improvements in treatments. Potassium disorders are referred as dyskalemia and they remain poorly characterized in heart failure patients. Potassium has been found to be an important biomarker to monitor since Heart Failure and related comorbidities, as well as the pharmacological treatments and comorbidities are likely to cause potassium alterations. In general, both low levels (hypokalemia) and high levels (hyperkalemia) of potassium can lead to life-threatening conditions. Clinical guidelines set the normal range of serum potassium between 3.5–5.0 mmol/L in the general population. However, recent studies have raised serious concerns about the validity of this range in patients affected by heart failure (**?**Ferreira *and others*, 2020). More importantly, the role of the dyskalemia dynamics needs to be explored and the concept of a fixed cut-off valid for all patients irrespective of their characteristics and measurements history needs to be revised.

In Section 2 we describe the proposed method, graphically summarized in Figure 1. Section 2.1

describes the representation and estimation of the biomarkers longitudinal trajectories while Section 2.2 is devoted to the landmark survival model. Section 3 provides details on the dataset used for the application. The results are given in Section 4. In Section 4.1 a general description of the cohort is given while in Section 4.2 the motivation for using the mixed-wavelet approach is discussed together with the details with regards to its implementation. The results of the survival model are shown in Section 4.3 while in Section 4.4 a possible clinical tool derived from the mixed-wavelet landmark model is proposed for the monitoring of potassium in the context of heart failure. The performance with regards to the predictive accuracy of the proposed method is reported and compared with the one obtained from the existing methods from the literature in Section 4.5. Finally, the discussion and conclusions are in Section 5. All analyses were performed in R and the code is available on https://github.com/caterinagregorio/MixedWaveletLandmark.

2. Methods

2.1 *Functional wavelet filter coupled with linear mixed models for continuous longitudinal data*

For each patient $i \in \{1, ..., n\}$, we let $Y_i(t)$ be the longitudinal biomarker profile and $y_{ij}, j = \{1, ..., m_i\}$ the repeated measurements observed for the subject i. We also denote by t_{ij} the corresponding measurements times and by y_{it^-} and t_{it^-} the value and the time of the last measurement before a generic time t respectively. For the individual biomarker trajectory we assume the following model:

$$Y_i(t) = L_i(t) + S_i(t) + \epsilon_i(t)$$

where $L_i(t)$ is the long-term trend component, $S_i(t)$ is the short-term component and $\epsilon_i(t)$ is the Gaussian measurement error term with mean 0 and variance σ^2_ϵ.

To estimate the long-term trend, $L_i(t)$, we specify a linear mixed effect model:

$$L_i(t) = (\boldsymbol{\alpha} + \mathbf{a}_i)f(t) + \tilde{\mathbf{x}}_i\tilde{\boldsymbol{\alpha}}$$

where $f(\cdot)$ is a possibly non-linear function of time, $\boldsymbol{\alpha}$ and $\tilde{\boldsymbol{\alpha}}$ are fixed-effect coefficients for time and baseline covariates respectively and $\mathbf{a}$ are the random effects coefficients.

The short term component is a non-parametric term which can be estimated using a wavelet Morlet filter (Carmona *and others*, 1998). Morlet wavelets are continuous, complex-valued functions used to smooth non-stationary time-series data and they allow to distinguish the frequencies at which oscillations occur. The Morlet wavelet transform is characterized by a "mother wavelet": $\Psi(t) = \pi^{-1/4}e^{6it}e^{-t^2/2}$. The estimation procedure consists of the following steps. First, the mixed effect model is fitted and the predicted values of the individual biomarker profile, $\hat{L}_i(t)$, on a suitable time-scale e.g. daily predictions are obtained.

On the other hand, a initial estimator for the short-term component, $S_i(t)$, is obtained using an interpolation of the residual individual trajectory as: $\tilde{S}_i(t) = y_{it^-} - \hat{L}_i(t)$. We can then use the Morlet wavelet transform on $\tilde{S}_i$. The Morlet wavelet transform is defined as the convolution of $\tilde{S}_i$ with a set of "wavelets daughters" obtained by translating the mother wavelet in time and scaling it by a frequency, f (Rösch *and others*, 2018):

$$Wave_i(\tau, f) = \sum_t \tilde{S}_i(t)\frac{1}{\sqrt{f}}\Psi^*\big(\frac{t-\tau}{f}\big)$$

where Ψ^* indicates the complex conjugate of Ψ. τ determines the position of a specific daughter wavelet in time while f is the frequency.

Instead of f, it can be equivalently defined the period $1/f$. The choice of the set of frequency to consider will determine the periods of the oscillations that are allowed in the short-term component e.g. the velocity of the short-term changes. From this transformation a new estimator for $S_i(t)$ can be derived as:

$$\hat{S}_i(t) = \frac{df dt^{1/2}}{0.776\Phi(0)} \sum_f \frac{Re[Wave_i(t,f)]}{f^{1/2}} \tag{2.1}$$

where *df* and *dt* are the frequency and time resolution chosen for the transform and $Re(\cdot)$ denotes the real part. However, in Equation 2.1 it is assumed that no measurement error is present which it not realistic in the case of biomarkers. For this reason, during the reconstruction a smoothing, or filter, is performed so that only relevant parts of the transform are retained and measurement error is removed. For the filtering, a criterion based on the wavelet power spectrum is used. The power spectrum is defined at a particular time and period as:

$$P_i(\tau, f) = \frac{1}{f}|Wave_i(\tau, f)|^2$$

where $|\cdot|$ stands for the modulus. The power spectrum corresponds to the square of the local amplitude of the corresponding wavelet transform component. In order to select which components $Wave_i(\tau, f)$ are to be kept in the estimation, we test the hypothesis H_0 corresponding to $P_i(\tau, f)$ being the power spectrum of a white noise process. Moreover, a minimum power level can be set according to a minimum sensibility that we want our estimated subject-specific biomarker profiles to have. Such minimum power level should be chosen according to our biological knowledge of the biomarker under study. Finally, to reduce false positives it can be sensible to exclude components whose period is smaller than the distance between τ and last measurement before τ. Indeed, if the null hypothesis was rejected for such components, it would be due to artifacts since it is impossible that changes over a period smaller than the distance from the previous measurement had happened. Therefore, the final estimate for $\hat{S}_i(t)$ becomes:

$$\hat{S}_i(t) = \frac{df dt^{1/2}}{0.776\Phi(0)} \sum_f \hat{\theta}_i^{\tau,f} \frac{Re[Wave_i(t,f)]}{f^{1/2}}$$

where $\hat{\theta}_i^{\tau,f} = \mathbb{1}(P_i(\tau, f) > min(P^\alpha(\tau, f), P_{min}) \wedge \tau - t_{i\tau^-} \geqslant 1/f)$, $P^\alpha(\tau, f))$ is the critical value of the test at α significance level and P_{min} is the minimum power level chosen. It is important

to note that $\hat{\theta}_i^{\tau,f}$ can also be 0 for $\forall\tau$, f. In the latter case the short-term component for subject i would be null and therefore $\hat{S}_i(t) \equiv 0$. Finally, we can also decide to reconstruct the short term component according to a subset of the frequencies considered in the wavelet transform.

2.2 *Landmark survival model*

We let T_i and C_i the individual's death and censoring time respectively. We assume that C_i is non-informative with respect to the biomarker process and death time. For each patients we only observe the couple $Z_i = min(T_i, C_i)$, $\delta_i = \mathbb{1}(T_i \leqslant C_i)$. When the interest lies in studying the association between internal time-dependent covariates and the risk of death, a conditional approach can be used. We can set a grid of time-points, called landmarks, in which information on the longitudinal covariate is updated. At each landmark point we can study the relationship between the covariate and time of death by estimating a Cox proportional hazard model using covariate information up to the landmark point. The dataset used for the estimation contains only patients still under observation at the landmark time. Moreover, the events up to a fixed time horizons are retained while patients experiencing the event after the horizon are censored at the horizon time. Let w be the time horizon and $h = \{h_1, ..., h_l\}$ the landmark times. To gain efficiency and interpretability, instead of estimating different models for each landmark time, we can specify a so called "landmark supermodel" (van Houwelingen and Putter, 2011):

$$h_i(t|\mathbf{z}_i, \mathbf{x}_i(\mathbf{h}), h, w) = h_{h,0} \exp\{\mathbf{z}_i\boldsymbol{\beta} + \mathbf{x}_i(\mathbf{h})\boldsymbol{\gamma}\}, h \leqslant t \leqslant h + w \tag{2.2}$$

where $\mathbf{z}_i$ is the vector of fixed covariate, $\mathbf{x}_i(\mathbf{h})$ is the vector of time-dependent covariate at time h and $\boldsymbol{\beta}$ and $\boldsymbol{\gamma}$ are the respective coefficients. The dataset used for the estimation is the one made by stacking all the datasets used for the separate landmark models. It is important to note that an event can appear in the "stacked" dataset more than once if is falls in the $h + w$ interval for more than a landmark point h. This is the reason why the robust sandwich estimator for the

standard errors is used.

2.3 *Wavelet-mixed landmarking*

In the classic landmark analysis as $\mathbf{x}_i\mathbf{(h)}$ the last observation before h is used (LOCF approach). We propose a novel approach using as $x_i(h)$ an estimation based on the method proposed in Section 2.1. Having the survival analysis in mind, summarizing the long-term and short-term information in one variable means assuming that the prognostic role of the different components is similar and it has the same importance. In general, this is a very strong assumption. For this reason we consider different short-term components according to the duration of the short-term oscillation we are interested to study. More precisely for each landmark time h and subject i, we obtain the vector $x_i(h)$ as follow:

- **STEP 1**: Obtain the predicted current value, $\hat{l}_i(h)$, and its first derivative (slope), $\hat{l}'_i(h)$, from the Linear Mixed Model at time h.
- **STEP 2**: Apply to the residual trajectory up to time h the Wavelet filter as described in Section 2.1.
- **STEP 3**: Reconstruct the short-term components at time h according to the set of durations of interest $(1/f_1, 1/f_2, \cdots, f_{max-1}, 1/f_{max})$:

$$\hat{S}_i(t)^{[1/f_1-1/f_2]}, \cdots, \hat{S}_i(t)^{(1/f_{max-1}-1/f_{max}]}$$

- **STEP 4**: For each short-term component a categorical variable can be also defined as follows:

$$\hat{O}_i(h)^{1/f_j-1/f_k} = \begin{cases} \text{“}upward\text{”} & \text{if } \hat{S}_i(h)^{1/f_j-1/f_k} > 0 \\ \text{“}downward\text{”} & \text{if } \hat{S}_i(h)^{1/f_j-1/f_k} < 0 \\ \text{“}no\text{”} & \text{if } \hat{S}_i(h)^{1/f_j-1/f_k} = 0 \end{cases}$$

2.4 *Biomarker related risk assessment*

In clinical practice, biomarker information is often used mainly through cut-offs which distinguish 'normal' values from 'abnormal' ones. On the other hand, it would be very useful to quantitatively assess how dangerous an individual biomarker trajectory observed up to a time, e.g. in correspondence of a clinical visit, is with respect to the risk of death. While being useful for a global assessment of the patient's prognosis, the dynamic prediction of the survival probability is not suitable to assess the impact on the risk of the patient's biomarker trajectory. For this reason, we propose a score based on statistically significant components of the the biomarker trajectories, which feeds a dynamic tool for supporting medical doctors daily practice. To obtain the score, the partial linear predictor, $\mathbf{x}_i''(h)\boldsymbol{\gamma}$, predicted for an individual i at time t is categorized in risk groups by using the observed quantiles in the entire cohort.

3. Dataset

The integration of administrative and Electronic Health Recording Systems offers new opportunities to elaborate prognostic models in a real-world context. Nowadays, these kind of data play an important role in extracting Real World Evidence that help to manage highly complex conditions such as patients in the cardiovascular setting. The data source used in this work is an example of such resources. Data was obtained by the interrogation of the administrative regional health data of Friuli Venezia Giulia Region in the Northern part of Italy, integrated with data derived from the Outpatient and Inpatient Clinic E-chart (Cardionet ®). This integrated database constitutes the Trieste Observatory of Cardiovascular Diseases and it represents one-of-a-kind case in Italy, where the integration of different data sources for clinical research is still limited and fragmented. Specifically, this was a cohort observational, non-interventional study involving patients living in the Trieste area who had an Heart Failure diagnosis between January 2009 and December 2020, had at least one cardiological evaluation, two potassium measurements and were

observed for at least one year. For the identification of the HF patients, the following steps will be followed. First, a search in the electronic medical records, using appropriate keywords (Heart Failure, Chronic Heart Failure, Systolic Heart Failure, Diastolic Heart Failure) to select patients with HF-related clinical findings. In order to avoid any diagnostic underestimation, data from the medical E-chart were combined with the discharge codes of any previous hospital access (based on the standard nomenclature of the ICD-9 CM) and/or interventional procedures for HF patients (i.e. ICD implantation). Subsequently, prospective cases were manually reviewed by clinicians, to validate the diagnosis of HF using the criteria established in 2016 by the European Cardiology Society. The cohort was followed from the index date, defined as date of first ambulatory visit with a potassium measure available, until the time of death or the end of the follow-up (administrative study closure date, fixed at 31 December 2020). The database has been previously described in the literature (Iorio *and others*, 2019). For this specific study demographic, clinical and instrumental variables at the index date together with all repeated blood tests containing the potassium measurements have been considered.

4. Results

4.1 *Study Cohort*

2981 subjects were included in the analysis. Their characteristics at the index date are summarized in Table 1. The median age in the cohort was 77 years (IQR: 70-83) and 58% were male. In median, they had a Left Ventricular Ejection Fraction (LVEF) of 54% (IQR: 40-63). LVEF is a measure of the heart function and it is considered to be normal when it is over 50%. In this cohort, 40% of patients had a reduced LVEF. The New York Heart Association (N.Y.H.A) class indicates the progression of heart failure. In this case, 88% of patients had a class of 1 or 2 corresponding to asymptomatic and mild symptoms respectively. Furthermore, 48% of patients had diagnosis of Chronic Kidney Disease (CKD) and 64% patients had more than 3 non-cardiac

comorbidities. The median time of follow-up period in the cohort was 55 months (IQR: 33-80 months). Finally, subjects had a median number of potassium measurements of 20 (IQR 11-36) at a median distance of 4 days (IQR: 1-32 days). At 2 years of follow-up, Kaplan-Meier estimate of the survival probability was equal to 0.92 (95%CI 0.91-9.93).

4.2 *Longitudinal potassium trajectories*

To explore the relationship between the risk of death and potassium (K) in Fig. 2 we show the trajectories of potassium observed for a random sample of 200 patients against the time to the end of the observation period. Patients have been divided in two groups: subjects who died and patients still alive at the end of the study. A lowess smoothing curve was used to compare the overall trajectory between the two groups. It can be observed that the lowess curve falls within the standard normality range of 3.5-5 mmol/L in both groups. Moreover, the lowess curves appear rather flat over time both in censored and in subjects who died even though the group with the event shows a slight decrease in potassium values just before the time of death. However, from the individual observed trajectories it can be observed how patients who died tend to exhibit an oscillatory pattern towards the end of the follow-up.

The linear mixed effects model has been fitted using the `lme` `R` function from the `nlme`(Pinheiro *and others*, 2021) package. Some of the factors which are known to influence potassium are age, sex, Chronic Kidney Disease and Heart Failure itself. For this reason these variables, measured at baseline, were used as covariates in the Linear Mixed Effect model (Table 2). Specifically, from the estimates of the fixed coefficients it seems that males have a higher mean potassium values, C.K.D seems to increases mean potassium values whereas a N.Y.H.A. class above 2 is associated with lower potassium values. A flexible dependence between overall mean trajectory and time was defined through a cubic b-spline with four degrees of freedom. Knots were placed at 25th, 50th and 75th percentile of the measurements times. Subject-specific changes in the potassium trajectory

are determined by disease progression as well as drugs intake, hospitalizations, worsening of the renal function. These are unobserved longitudinal processes and their effect on potassium can be taken into account using time related random effects. We used a cubic b-spline with four degrees of freedom for the random effects as well to allow for the estimated individual potassium trajectories to be as flexible as possible. In Fig.3 the predicted mean trajectories are shown for the same sample of 200 subjects previously displayed. Compared to the observed trajectories, the predicted one from the linear mixed model appear to be flatter. Indeed, when residuals are plotted against time (Fig.4), they are not scattered at random as they should. Although a flexible function of time was used for the random effects, the model's goodness of fit is not satisfactory. To inspect the serial correlation still present in the data, we can use the empirical semi-variogram for the within-subject residuals obtained from the model (Fig.5). From the semi-variogram we can observe that dependence is present and the range of influence of potassium measurements seems to be close to six months.

To retrieve the individual short-term oscillations, we used the methods introduced in Section 2.1 and the `WaveletComp` (Rösch *and others*, 2018) package in `R`. The range of periods considered for the wavelet transform was 2-365 days and the minimum level for the power spectrum allowed for the component to be included in the reconstruction was 0.09. An example of the estimated potassium trajectory obtained as $\hat{L}_i(t)+\hat{S}_i(t)^{2-365}$ for one patient shown in the top panel of Fig.6. We can observe how the estimated long-term trend is rather flat. Through the wavelet filtering, we were able to identify the short-term oscillations. In the bottom panel of Fig.6 is shown the periodogram which represents the power spectrum defined as in Equation 2.1 corresponding to time points τ (x-axis) and period $1/f$ (y-axis). As reflected in the estimated $\hat{s}_i^{2-365}(t)$, the strongest changes are present just before 2 years of follow-up and after the fifth year and their length is between 90-180 days and 14-30 days respectively.

4.3 *Survival Model Results*

As landmark points we considered time points from 1 to 5 years at a distance of 90 days. The time horizon was fixed at 6 months. Following the steps described in Section 2.3, we obtained $\hat{S}_i(h)^{[2-14]}$, $\hat{S}_i(h)^{(14-30]}$, $\hat{S}_i^{(30-90]}(h)$, $\hat{S}_i(h)^{(90-180]}$, $\hat{S}_i(h)^{(180-365]}$. The rationale behind this choice was the clinical interpretation of the short-term components. These intervals were discussed with the clinical experts involved in the study and they reflects clinical practice routines. More specifically, potassium measurements are usually repeated within 14 days and again after 30 days during up-tritation of the pharmacological treatments or more frequently when patients are hospitalized. In both cases these can be considered possible reasons for "acute crisis" in the values of potassium. On the other hand, 90, 180 and 365 days are the intervals where patients can be reevaluated by cardiologists and when effects of disease progression or worsening of comorbidities (e.g. chronic kidney disease) on potassium can be observed.

Two sets of covariates for the representation of the individual potassium trajectories were considered:

$$\mathbf{x}_i'(h) = \begin{bmatrix} \hat{l}_i(h) & \hat{l}_i'(h) & \hat{s}_i(h)^{[2-14]} & \hat{s}_i(h)^{(14-30]} & \hat{s}_i(h)^{(30-90]} & \hat{s}_i(h)^{(90-180]} & \hat{s}_i(h)^{(180-365]} \end{bmatrix}$$

$$\mathbf{x}_i''(h) = \begin{bmatrix} \hat{l}_i(h) & \hat{l}_i'(h) & \hat{o}_i(h)^{[2-14]} & \hat{o}_i(h)^{[15-30)} & \hat{o}_i(h)^{(30-90]} & \hat{o}_i(h)^{(90-180]} & \hat{o}_i(h)^{(180-365]} \end{bmatrix}$$

$\mathbf{x}_i'(h)$ contains the continuous version of the variables for the short-term oscillations whereas $\mathbf{x}_i''(h)$ contains their categorical versions. A model for each set of time-dependent covariates was fitted using the `R survival` package (Terry M. Therneau and Patricia M. Grambsch, 2000; Therneau, 2022). The one with the categorical variables had the lowest AIC and it therefore was chosen. The results are shown in Table 3. Older age, N.Y.H.A. class>2 and a reduced ejection fraction at baseline are associated with an increased risk of death. Since both low and high values

of potassium are believed to be dangerous, the long-term trend is allowed to have a non-linear effect on the hazard through a cubic regression spline with 4 degrees of freedom (internal knots were placed at 25th, 50th and 75th percentiles of the distribution). Interestingly, neither the current value nor the slope of the long-term trend appear to be significantly associated with the risk of death. The latter can be explained by the fact that the individual long-term trends appear to be rather flat in this population. On the other hand, the presence of short-term oscillations up to the period (180-365] days have an impact on the risk of death. Therefore, the history of the longitudinal process seems to influence the survival up to 1 year. Last, both downward and upward oscillations increase the risk of death. This aspect is clinically motivated by the fact that changes in potassium are dangerous in both directions.

4.4 *Predictive performance*

We have compared the predictive accuracy of the proposed model (M) with the existing ones from the literature through discrimination and calibration. Specifically, as measures of calibration and discrimination we used the Dynamic Area Under the Curve (AUC(t)) and the Brier Score. The methods considered for the comparison were the following:

- **CM1** Landmark survival model with the last observed measurement of potassium as $x_i(h)$;
- **CM2** Landmark survival model with the last observed measurement of potassium treated as categorical variable using the cut-off currently used in the clinical practice $x_i(h)$:

$$x_i(h) = \begin{cases} \text{“}normal\text{”} & \text{if } 3.5\text{mmol/L} \leqslant y_{it^-} \leqslant \text{mmol/L} \\ \text{“}hyperkalemia\text{”} & \text{if } y_{it^-} > 5\text{mmol/L} \\ \text{“}hypokalemia\text{”} & \text{if } y_{it^-} < 3.5\text{mmol/L} \end{cases}$$

- **CM3** Mixed landmark survival model with $\mathbf{x}_i(h) = [\hat{l}_i(h) \quad \hat{l}'_i(h)]$, i.e. current value and slope

- **CM4** Joint model with the current value and slope parametrization.

The specification of the linear mixed effect in models CM3 and CM4 was the same of the one described in Section 4.2.2. Similarly, the fixed covariates in the Cox's survival model were the same as the one described in Section 4.3. CM4 was fitted using the `JMBayes` package (Rizopoulos, 2016). 10-folds cross validation was used to obtain both the indices and the prediction horizon considered was 6 months. For the definition of AUC(t) and the Brier Score the one proposed by Blanche *and others* (2015) was used. In Fig.7 it can be observed that proposed method has the highest calibration and discrimination. Interestingly, models CM3 and CM4 appears to be the worst. Indeed, they rely only on the long-term trend for the representation of the individual potassium trajectories which does not contain prognostic information in this case.

4.5 *Heart Functional Dynamic potassium(K) Score*

In Heart Failure, the monitoring of potassium plays an important role. Therefore, a score which could easily be used by cardiologist would be very useful to quantitatively assess the patient's risk using the potassium measurements available. For this reason, using the method explained in Section 2.4, we propose the Heart Functional Dynamic potassium(K). The score is categorized into four risk groups by using the observed quartiles in the entire cohort. A fifth category corresponds to no short-term oscillations at time t. Fig.8 shows an example of a patient's predicted survival probability dynamically updated at times 1, 1.2, 1.7, 2.2 and 4.7 together with the corresponding predicted HFDKS. It can be observed how at 1 year, while having the last potassium value over 5 mmol/L, the patients is at low risk. The risk becomes very high at 1.7 years after the subject has experienced multiple oscillations. At time=2.2 days of follow-up the score decreases as short-term oscillations seem to have stopped and the potassium has stabilized around 4 mmol/L. At time 4.7 the risk is predicted to be high again because of a new crises happening. As expected, the predicted 6-months survival probability shows a similar pattern with lower probability of survival

in the following 6 months at 1.7 and 4.7 years of follow-up.

5. Discussion & Conclusions

In this paper, we proposed a novel method to study the relationship between a continuous longitudinal biomarker and survival based on landmarking. Specifically, the focus of our method is to provide a mathematical representation of the individual biomarkers profiles allowing for the presence of short-term oscillations. Internal time-varying covariates require methods which allows to take into account measurement error as well as to consider the history of the longitudinal process up to a specific time. However, the existing methods addressing these points have focused on mixed-effects models which have severe limitations when the subjects' observation period time span over years. Indeed, in linear mixed models the local variation is captured in the error term and it is therefore lost. We claim that the residual serial correlation has a prognostic role since it corresponds to short-term oscillations. Such oscillations represents "crises" due to other unobserved internal time-dependent variables. This issue can't be solved by simply considering a more flexible specification of the mixed-effects model because the short-term oscillations have not a common structure across subjects but they vary across individuals both in terms of timing and duration.

To overcome this problem, we proposed a novel method which combines linear mixed effect modeling coupled with a functional approach based on wavelets filters. The linear mixed model allows to capture the effect of baseline covariates and the subject-specific long-term profiles while the functional approach on the residuals allows to identify the individual short-term oscillations at different timings and of different duration. Functional Data Analysis techniques such as Functional Principal Component Analysis (FDA) have been proposed to include time-dependent covariates for dynamic prediction in survival models (Yao, 2007; Shi *and others*, 2021. In this work we have shown with a novel approach the capability of FDA as a method to effectively represent

biomarker time-dependent covariates.

Our work was motivated by a clinical problem in patients affected by Heart Failure. In this disease it is very important to monitor potassium since it is often altered by the disease as well as by pharmacological treatments. The relationship between potassium and survival in Heart Failure remains debated and the role of its dynamics over time has not been studied yet. Currently, in the clinical practice normality cut-offs on a single measurement are the only available quantitative method to assess patients' situation with regards to potassium. The proposed method enabled to show the prognostic role of short-term oscillations as well as providing the basis for a dynamic score to quantitatively summarise the risk of death associated with the observed history of potassium measurements. This is an important point since the goal of this work was also to provide a possible solution for the problem of monitoring of potassium in the clinical practice. In the context of the application presented, we compared the performance of our method with standard landmarking, a mixed-landmark model and a joint model. From this comparison, it is clear that a correct mathematical representation of the longitudinal process in very important. The two methods that should perform best (the joint model and the mixed landmark survival model) are worse than the models that disregard measurement error. The reason is that they both consider only the long-term component of the potassium trajectories which in this case it is not the relevant part of the longitudinal process from a prognostic point of view. On the contrary, the mixed-wavelet approach recovers the short-term oscillations and improves the performance of the survival model.

The proposed method could also be applied to other clinical settings involving long-term monitoring of biomarkers. Moments of crises in biomarkers translating in short-term oscillations can be quite common in chronic diseases and our approach can help studying their role in a time-to-event setting. Specifically, the method is flexible in the definition of what short-term means as well as in the definition of the time-dependent covariates representing the short-term oscillations. Both

the choice of the maximum period to consider for the short-term oscillation and the intervals for the dimensionality reduction of periodogram with respect to the frequency domain can be chosen according to the biological knowledge and sample size considerations.

Finally, in studying the relationship between a longitudinal process and a time-to-event process a very important aspect consists in the dependence of the survival process from the biomarker's past. An additional novelty of our method is that it allows to explore how much of the history of the longitudinal process is relevant for the time-to-event process.

In this work the long-term component and the short-term components are estimated in two steps. In the future it could be of interest to develop a method to obtain them simultaneously following recent developments in frequency decomposition of multiple time-series data using Bayesian modelling (Hart *and others*, 2022; Costafreda *and others*, 2009; Cadonna *and others*, 2019).

6. Software

Software in the form of R code, is available on https://github.com/caterinagregorio/MixedWaveletLandmark.

Acknowledgments

This work was supported by VIFOR Pharma. The authors also thank the Trieste Observatory of Cardiovascular Disease, Dr.Andrea Di Lenarda and Dr.Arjuna Scagnetto. *Conflict of Interest*: None declared.

References

Blanche, Paul, Proust-Lima, Cécile, Loubère, Lucie, Berr, Claudine, Dartigues, Jean François and Jacqmin-Gadda, Hélène. (2015, mar). Quantifying and comparing dynamic predictive accuracy of joint models for longitudinal marker and time-to-event in presence of censoring and competing risks. *Biometrics* **71**(1), 102–113.

Cadonna, Annalisa, Kottas, Athanasios and Prado, Raquel. (2019, oct). Bayesian Spectral Modeling for Multiple Time Series. *Journal of the American Statistical Association* **114**(528), 1838–1853.

Carmona, R., Hwang, W.-L. and Torresani, B. (1998). *Gabor and Wavelet Transforms with an Implementation in S*, 1st Editio edition. Academic Press.

Costafreda, Sergi G., Barker, Gareth J. and Brammer, Michael J. (2009, may). Bayesian wavelet-based analysis of functional magnetic resonance time series. *Magnetic Resonance Imaging* **27**(4), 460–469.

Ferreira, João Pedro, Butler, Javed, Rossignol, Patrick, Pitt, Bertram, Anker, Stefan D., Kosiborod, Mikhail, Lund, Lars H., Bakris, George L., Weir, Matthew R. and Zannad, Faiez. (2020). Abnormalities of Potassium in Heart Failure: JACC State-of-the-Art Review. *Journal of the American College of Cardiology* **75**(22), 2836–2850.

Ferrer, Loïc, Putter, Hein and Proust-Lima, Cécile. (2019, dec). Individual dynamic predictions using landmarking and joint modelling: Validation of estimators and robustness assessment. *Statistical methods in medical research* **28**(12), 3649–3666.

Hart, Brian, Guindani, Michele, Malone, Stephen and Fiecas, Mark. (2022, mar). A nonparametric Bayesian model for estimating spectral densities of resting-state EEG twin data. *Biometrics* **78**(1), 313–323.

Iorio, Annamaria, Sinagra, Gianfranco and Di Lenarda, Andrea. (2019, jun). Administrative database, observational research and the Tower of Babel.

Nason, Guy P. and Von Sachs, Rainer. (1999). Wavelets in time-series analysis. *Philo-*

sophical Transactions of the Royal Society of London. Series A: Mathematical, Physical and Engineering Sciences **357**(1760), 2511–2526.

Papageorgiou, Grigorios, Mauff, Katya, Tomer, Anirudh and Rizopoulos, Dimitris. (2019, mar). An overview of joint modeling of time-to-event and longitudinal outcomes.

Pinheiro, Jose, Bates, Douglas, DebRoy, Saikat, Sarkar, Deepayan and R Core Team. (2021). *nlme: Linear and Nonlinear Mixed Effects Models*.

Ramsay, J. O. and Silverman, B. W. (2005). Functional Data Analysis.

Rizopoulos, Dimitris. (2016). The R package jmbayes for fitting joint models for longitudinal and time-to-event data using MCMC. *Journal of Statistical Software* **72**(7).

Rizopoulos, Dimitris, Molenberghs, Geert and Lesaffre, Emmanuel M.E.H. (2017, nov). Dynamic predictions with time-dependent covariates in survival analysis using joint modeling and landmarking. *Biometrical Journal* **59**(6), 1261–1276.

Rösch, Angi, Schmidbauer, Harald, Roesch, Angi and Schmidbauer, Harald. (2018). WaveletComp: Computational Wavelet Analysis. pp. 1–38.

Shi, Bin, Wei, Peng and Huang, Xuelin. (2021, feb). Functional principal component based landmark analysis for the effects of longitudinal cholesterol profiles on the risk of coronary heart disease. *Statistics in Medicine* **40**(3), 650–667.

Terry M. Therneau and Patricia M. Grambsch. (2000). *Modeling Survival Data: Extending the Cox Model*. New York: Springer.

Therneau, Terry M. (2022). *A Package for Survival Analysis in R*.

Tsiasis Anastasios A. and Davidian Marie. (2004). JOINT MODELING OF LONGITUDINAL AND TIME-TO-EVENT DATA: AN OVERVIEW on JSTOR. *Statistica Sinica* **14**(3), 809–834.

Unser, Michael and Aldroubi, Akram. (1996). A review of wavelets in biomedical applications. *Proceedings of the IEEE* **84**(4), 626–638.

van Houwelingen, Hans C. and Putter, Hein. (2011). *Dynamic prediction in clinical survival analysis*, 1st Editio edition.

Yao, Fang. (2007). Functional principal component analysis for longitudinal and survival data. *Statistica Sinica* **17**(3), 965–983.

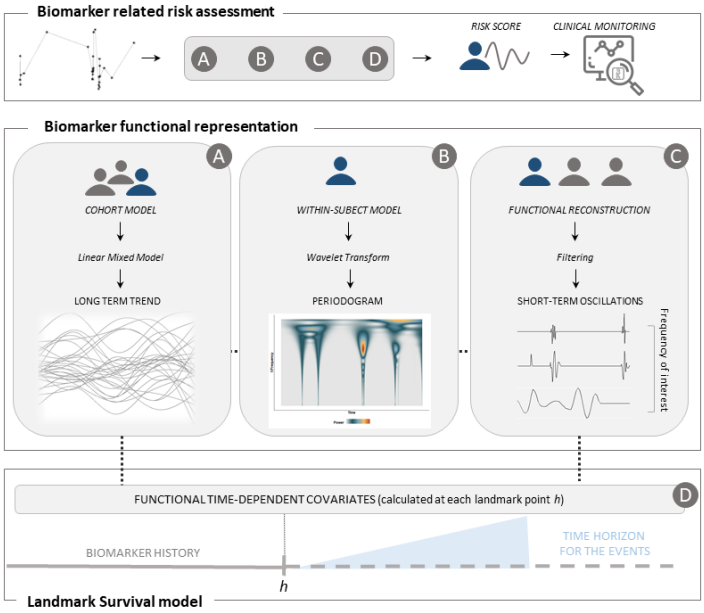

Fig. 1. Summary of the wavelet-mixed landmark survival method.

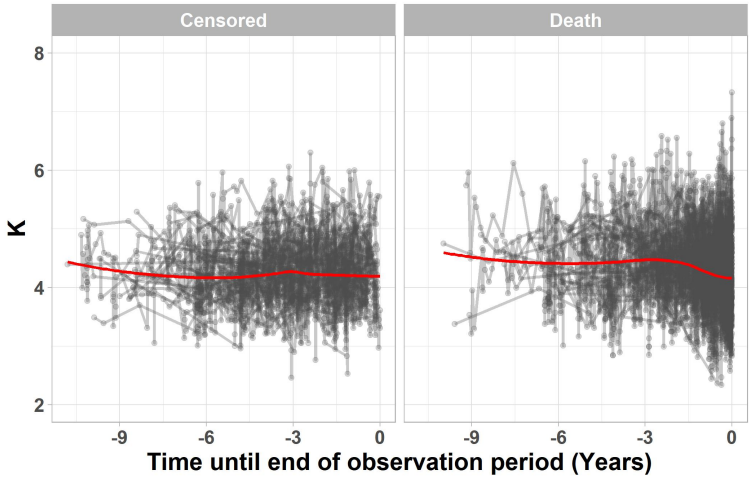

Fig. 2. Potassium measurements in a random sample of 200 patients in reverse time according to whether patients died (right panel) or they were censored (left panel). The red lines indicate the lowess smoothing curve.

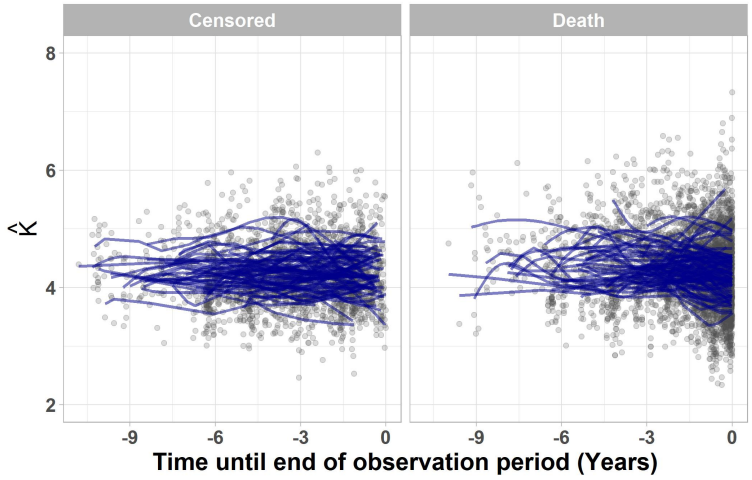

Fig. 3. Mean individual potassium trajectories in reverse time estimated with a linear mixed effects model in a random sample of 200 patients according to whether patients died (right panel) or they were censored (left panel)

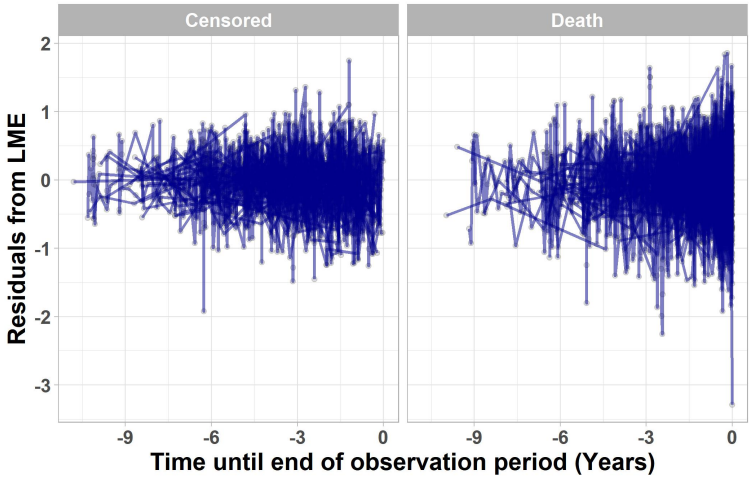

Fig. 4. Residuals obtained from the linear mixed effects model against reverse time in a random sample of 200 patients according to whether patients died (right panel) or they were censored (left panel)

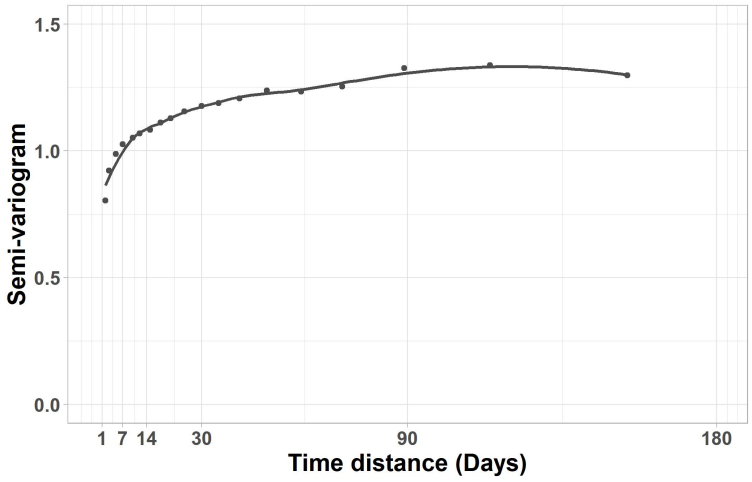

Fig. 5. Semi-variogram for the within-subject residuals.

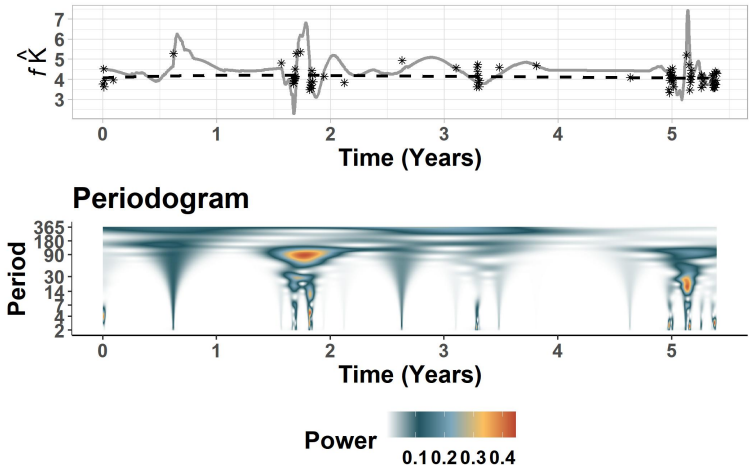

Fig. 6. **Top panel**: Example of the estimated functional potassium trajectory (grey line) obtained through wavelet filtering and mixed-effects model (black dashed line) in one patient. **Bottom panel**: corresponding periodogram obtained through the wavelet transform.

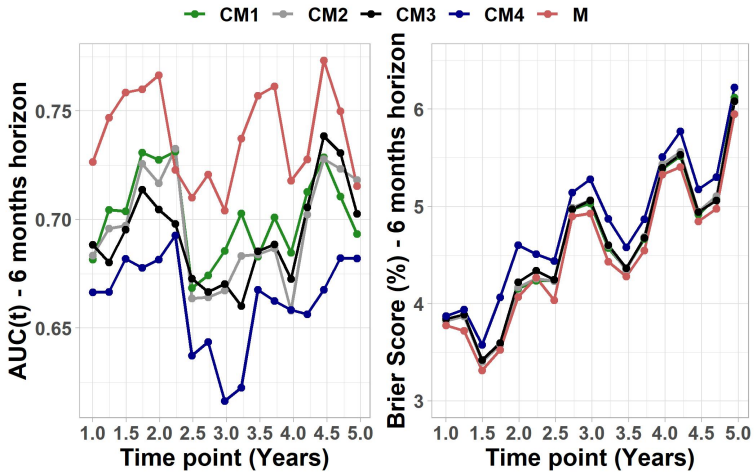

Fig. 7. Discrimination (left panel) and calibration(right panel) obtained used 10-folds cross validation.

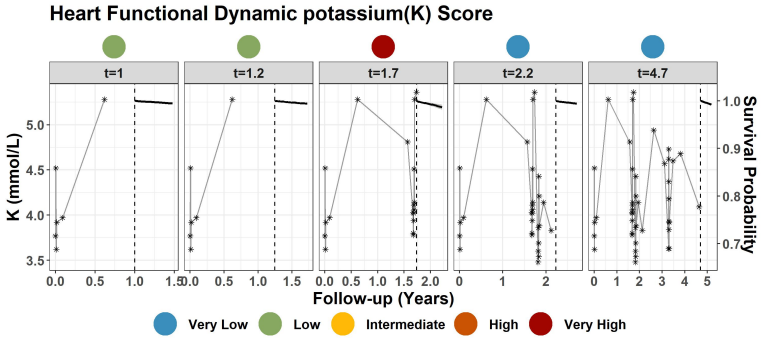

Fig. 8. Example of dynamic prediction for one patient's HFDKS and corresponding 6-months survival probability.

Table 1. *Descriptive statistics of the cohort.*

Characteristic	n = 2,981
Age, years	77 (70, 83)
Gender, male	1,730 (58%)
LVEF, %	54 (40, 63)
LVEF class	
HFpEF	1,780 (60%)
HFrEF	1,201 (40%)
NYHA Class	
1	1,102 (37%)
2	1,516 (51%)
3	337 (11%)
4	26 (0.9%)
CKD	1,422 (48%)
Non-cardiac comorbidities > 3	1,915 (64%)
Number of potassium measurements	20 (11, 36)
Median (IQR); n (%)	

Table 2. *Estimates of the linear mixed-model fixed coefficients along with standard errors, p-value and 95% confidence intervals.*

Variable	Coefficient	Std. Error	p-value	95% CI
Intercept	4.14	0.01	<0.001	4.11;4.16
Sex, Male	0.06	0.01	<0.001	0.04;0.08
Age	-0.01	0.01	0.3197	-0.02;0.01
CKD	0.12	0.01	<0.001	0.1;0.15
N.Y.H.A. class > 2	-0.05	0.02	0.0014	-0.09;-0.02
B_1(time)	0.03	0.02	0.0968	0.001;0.06
B_2(time)	-0.02	0.03	0.4689	-0.08;0.04
B_3(time)	0.09	0.04	0.0183	0.01;0.16
B_4(time)	-0.17	0.08	0.0307	-0.32;-0.02

Table 3. *Estimates of the landmark survival model along with robust standard errors, p-value and 95% confidence intervals.*

Variable	Coefficient	Robust Std.Error	p-value	95% CI
Age	0.67	0.05	<0.0001	0.57;0.77
Sex, male	0.33	0.07	<0.0001	0.19;0.47
N.Y.H.A class >2	0.58	0.09	<0.0001	0.41;0.75
HFrEF (vs. HFpEF)	0.16	0.07	0.0196	0.03;0.30
Number of comorbidities>3	0.38	0.08	<0.0001	0.23;0.53
$B_1(\hat{l}(h))$	-0.26	062	0.6766	-1.47;0.96
$B_2(\hat{l}(h))$	-0.35	0.40	0.37676	-1.12;0.43
$B_3(\hat{l}(h))$	-0.44	1.33	0.7404	-3.04;2.16
$B_4(\hat{l}(h))$	-0.02	0.56	0.776	-1.11;1.08
Slope $\hat{l}(h)$	-0.01	0.03	0.8186	-0.05;0.04
$\hat{o}_i(h)^{[2-14]}$:				
Upward	0.52	0.17	0.0019	0.19;0.86
Downward	0.13	0.17	0.4446	-0.21;0.47
$\hat{o}_i(h)^{(14-30]}$:				
Upward	0.36	0.13	0.0040	0.11;0.6
Downward	0.49	0.12	<0.0001	0.26;0.72
$\hat{o}_i(h)^{(30-90]}$:				
Upward	0.59	0.09	<0.0001	0.4;0.77
Downward	0.64	0.09	<0.0001	0.45;0.82
$\hat{o}_i(h)^{(90-180]}$:				
Upward	0.12	0.09	0.1895	-0.06;0.3
Downward	0.31	0.09	0.0004	0.14;0.48
$\hat{o}_i(h)^{(180-365]}$:				
Upward	0.14	0.08	0.0719	-0.01;0.29
Downward	0.22	0.08	0.0043	0.07;0.37

MOX Technical Reports, last issues

Dipartimento di Matematica
Politecnico di Milano, Via Bonardi 9 - 20133 Milano (Italy)

47/2022 Botti, M.; Di Pietro, D.A.; Salah, M.
A serendipity fully discrete div-div complex on polygonal meshes

45/2022 Franco, N.; Fresca, S.; Manzoni, A.; Zunino, P.
Approximation bounds for convolutional neural networks in operator learning

46/2022 Lucca, A.; Fraccarollo, L.; Fossan, F.E.; Braten, A.T.; Pozzi, S.; Vergara, C.; Muller, L.O.
Impact of pressure guidewire on model-based FFR prediction

44/2022 Peli, R.; Dovera, L.; Fighera, G.; Menafoglio, A.; Secchi, P.
Forecasting Oil Production Rates in Primary Depletion using the Physics-based Residual Kriging functional approach

43/2022 Zappon E.; Manzoni A.; Gervasio P.; Quarteroni A.
A reduced order model for domain decompositions with non-conforming interfaces

40/2022 Fumagalli, A.; Patacchini, F. S.
Well-posedness and variational numerical scheme for an adaptive model in highly heterogeneous porous media

42/2022 Gatti, F.; Fois, M.; de Falco, C.; Perotto, S.; Formaggia, L.
Parallel simulations for fast-moving landslides: space-time mesh adaptation and sharp tracking of the wetting front

41/2022 Arnone, A.; Ferraccioli, F.; Pigolotti, C.; Sangalli, L.M.
A roughness penalty approach to estimate densities over two-dimensional manifolds

39/2022 Ferro, N.; Perotto, S.; Gavazzoni, M.
A new fluid-based strategy for the connection of non-matching lattice materials

38/2022 Burzacchi, A.; Landrò, M.; Vantini, S.
Object-oriented Classification of Road Pavement Type in Greater Maputo from Satellite Images